

DESIGN SPACE EXPLORATION OF HEMI-TOROIDAL FUSED QUARTZ SHELL RESONATORS

Mohammad H. Asadian, Yusheng Wang, Radwan M. Noor, Andrei M. Shkel
MicroSystems Laboratory, University of California, Irvine, CA, USA
Email: {asadianm, yushengw, rmmohamm, andrei.shkel}@uci.edu

Abstract—This paper discusses the selection of parameters for the geometry of micro glass-blown hemi-toroidal Fused Quartz (FQ) resonators. Comprehensive Finite Element (FE) simulations were performed to explore the design space of the shell resonators, focusing on frequency scaling of the operational resonance mode and the spurious resonance modes (tilt, rocking, out-of-plane, and torsional), as a function of shell geometry. It was demonstrated that a separation between resonance frequencies and mode-ordering can be achieved through optimization of the shell geometry at the different range of frequencies.

I. INTRODUCTION

3D Fused Quartz (FQ) shells offer mass, stiffness, and damping symmetry, as well as structural rigidity, for the sensing element of Coriolis Vibratory Gyroscopes (CVG). A precisely machined and polished hemispherical shell is the core of a Hemispherical Resonator Gyroscope (HRG) [1], and has motivated pursuing of the batch fabrication and miniaturization of 3D shell resonators, using Micro Electro-Mechanical Systems (MEMS) fabrication techniques.

Micro-glassblowing [2] and blow-torch molding [3] processes utilize the thermoplastic bulk deformation at temperatures above the FQ softening point to fabricate 3D shell resonators. In the former case, a cavity is etched in an FQ wafer and encapsulated by FQ-to-FQ plasma-assisted wafer bonding. At the glassblowing temperature, the pressure inside an encapsulated cavity builds up, and viscosity of FQ decreases. The encapsulated cavity expands and forms a 3D axisymmetric geometry with a self-aligned stem. Fig.1 shows an array of 3D FQ shells, demonstrating scalability of the fabrication process. Shell resonators with a broad range of operating frequency can be fabricated using the micro-glassblowing process [4].

Unlike vibration systems with lumped masses and discrete stiffness elements, shells are continuous systems with distributed mass and elasticity. Thus, they have an infinite number of orthogonal modes of vibration. Fig. 2 shows six vibrational modes of a typical hemi-toroidal shell. The Coriolis coupling between the degenerate wineglass (WG) modes can be configured to measure the rotation rate (rate gyro) or the

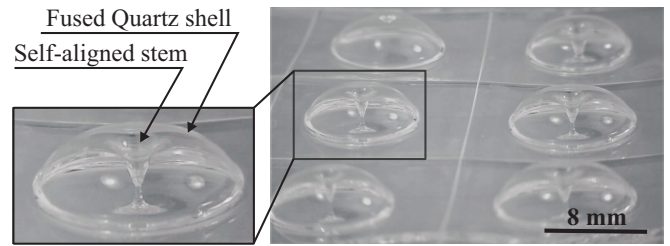


Fig. 1. An array of Fused Quartz shells fabricated using the high-temperature micro glassblowing process.

absolute angle of rotation (whole angle gyro) along the axis of symmetry of shell resonators. Thus, any wineglass resonance modes can be considered as the operational mode in 3D micro wineglass resonator gyroscopes, however the $n=2$ is considered to be a preferable structural mode for operation.

In this paper, the scaling of frequency in wineglass, tilt, torsional, and out-of-plane modes with respect to the shell radius, thickness, and anchor radius were analyzed using the Finite Element (FE) modal analysis. The results of the FE simulations were utilized to define a design space for hemi-toroidal shell resonators in a broad range of operational frequencies. The frequency separation between the $n=2$ WG mode and the closest parasitic mode was selected as the design parameter. In some cases, it was observed that the mode-ordering condition, where all the parasitic modes have higher resonance frequencies in comparison to the $N=2$ WG mode, was achieved through the design of shell geometry.

II. FREQUENCY SCALING OF 3D SHELL VIBRATION MODES

The resonant frequency of $n\theta$ wineglass modes of a hemi-toroidal shell was approximated analytically based on the Rayleigh's energy method [5]. In a hemi-toroidal shell with a uniform thickness, the wineglass frequency is linearly proportional to the thickness and inversely proportional to the square of the diameter. A parametric FE modal analysis was performed to derive the frequency scaling of spurious modes. An FQ shell geometry was approximated by a hemi-toroid shape for simulations. In simulations, it was assumed that the shell is fully developed and that the thickness is uniform.

This material is based on work supported by the Defense Advanced Research Projects Agency under Grant N66001-16-1-4021.

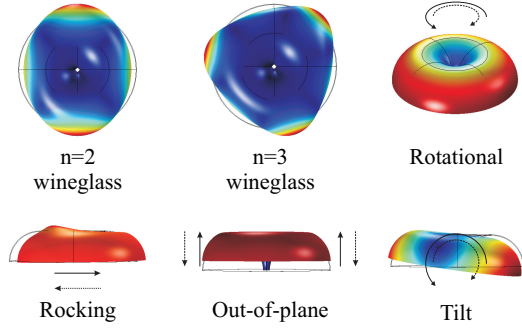


Fig. 2. The first six resonance modes of a typical hemi-toroidal shell structure, any degenerate wineglass modes can be used for rotation sensing, however the $n=2$ mode is preferable due to a higher gain in the whole angle mode of operation.

The scaling of resonance frequencies are plotted in Fig. 3. For a constant anchor radius and thickness, Fig. 3a, the frequency of all resonance modes decreases when the shell radius is increased. Fig. 3b shows the effect of shell's thickness on the resonance frequencies with a constant shell and anchor radius. The different scaling of resonance frequencies with shell thickness switched the order of resonance modes at certain geometries. A similar trend was observed with anchor radius, Fig. 3c. A larger anchor radius resulted in a higher torsional resonance frequency, while the wineglass and out-of-plane modes were nearly insensitive to the size of the anchor. Similar trends were observed in other combinations of the shell radius, anchor radius, and thickness. The FE modal simulation results indicated that:

- The resonance modes scale differently with respect to geometrical parameters of the hemi-toroidal shell.
- The frequency separation between the $n=2$ wineglass mode and spurious mode changed with shell geometry.
- The order of the resonance modes switched at certain geometries.

Based on the observations, the mode separation between the resonance modes can be designed to avoid the dissipation of energy through mode mixing [6], and the environmental sensitivity can be improved by avoiding low-frequency spurious resonance modes.

III. 3D SHELL DESIGN SPACE

The shell radius, thickness, and anchor radius are the design parameters that define the geometry of a hemi-toroidal shell. Using a parametric FE modal analysis, the shell thickness, radius, and anchor diameter were varied from $40\ \mu\text{m}$ to $150\ \mu\text{m}$, $2.5\ \text{mm}$ to $5\ \text{mm}$, and $100\ \mu\text{m}$ to $500\ \mu\text{m}$, respectively, generating more than 200 design combinations. The wineglass resonance frequency and the frequency separation with the closest parasitic mode at different design points are plotted in Fig. 4. Each data point refers to a distinct shell geometry, forming the design space for the geometry of hemi-toroidal shell resonators. The data points demonstrate that for a wineglass frequency of interest, a shell resonator can be designed

with a different combination of parameters. The separation between spurious and operational modes depends on selection of the geometric parameters. Also, we concluded it would be possible to design a shell resonator with spurious modes at higher resonance frequencies as compared to the $n=2$ WG mode, which is an important consideration for avoiding the environmental excitation of the device. The latter is the design to achieve ordering of modes. The red data points in Fig. 4 refer to cases where the mode-ordering condition is satisfied, and $n=2$ wineglass mode has the lowest resonance frequency.

A lower operational frequency of shell resonators relaxes the minimum capacitive gap requirement for electrostatic frequency tuning when the shell resonator is instrumented to operate as a mode-matched gyroscope [7]. However, the trend of data points revealed that the modal frequency separation decreases at lower operational frequencies. Thus, the shell geometry should be optimized to avoid proximity of spurious modes to the $n=2$ WG mode. A set of parameters corresponding to data points between 4 to 5 kHz for $n=2$ WG resonance are listed in Table I. The modal frequency separation varies from 610 Hz to 3.8 kHz for the chosen set of parameters.

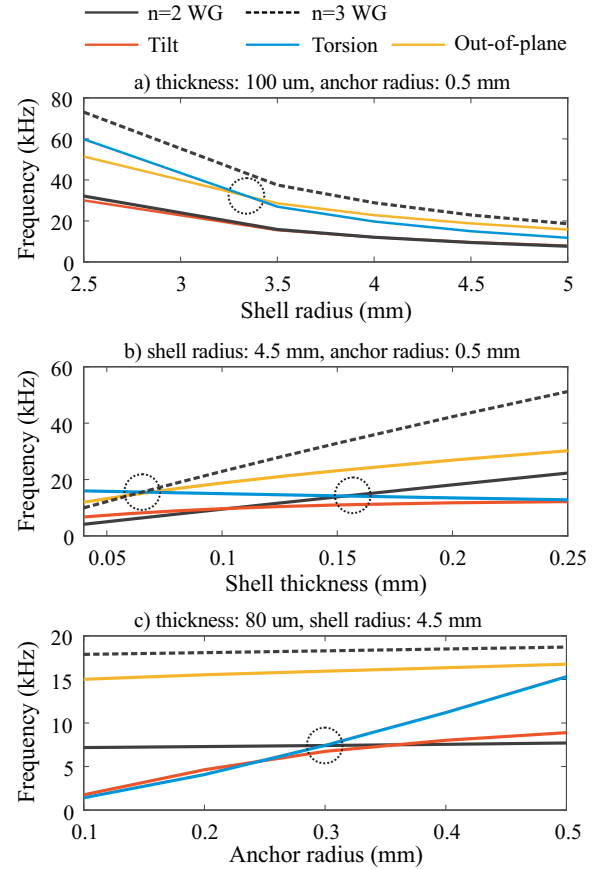


Fig. 3. Scaling of the resonance frequencies with respect to the geometry of hemi-toroidal shell resonators. Notice, the order of structural modes can switch at certain geometries. Circles indicate the geometries that the order of $n=2$ wineglass mode and its closest spurious modes changes.

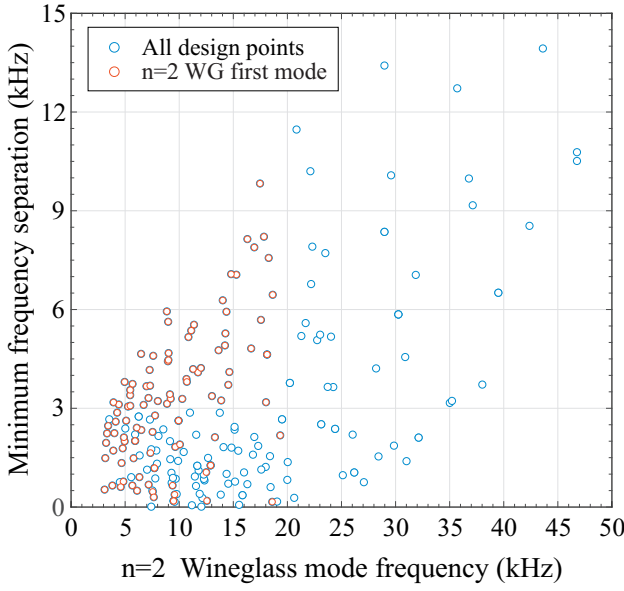


Fig. 4. The design space of hemi-toroidal shell resonators; frequency separation between the operational and the closest spurious modes at different $n=2$ WG resonance frequencies. Each data point represents a distinct shell geometry. The red points represent the design points where the $n=2$ WG is the lowest resonance mode (we call it mode-ordered).

IV. DETERMINATION OF PARAMETERS

The design space provides a set of parameters for the final shell geometries at the frequency of interest. However, the FQ material undergoes a large deformation during the glassblowing process to form a 3D shell structure from a flat die. The thickness of shell changes as the shell deforms until it fully develops during the glass blowing process and forms the final geometry. Therefore, it is crucial to determine initial thicknesses of FQ die, before glassblowing, to achieve the intended final geometry.

A shell deformation in the micro-glassblowing process was simulated using a time-dependent Newtonian isothermal fluid flow model with adaptive remeshing, using COMSOL Multiphysics FE Package [4]. The FE simulations were performed to predict the final thickness of the shell from their initial geometric parameters. The thickness was evaluated at the shell's

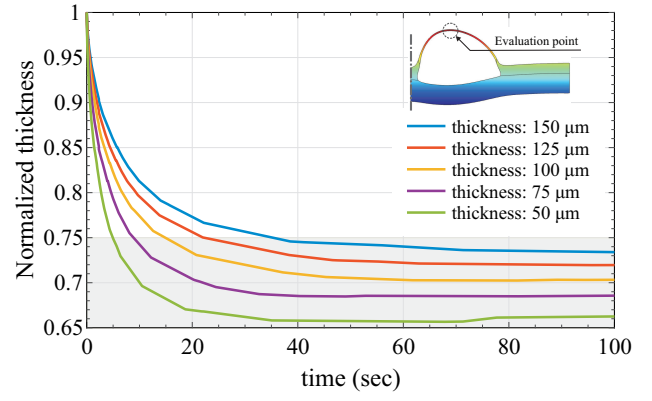


Fig. 5. 25% to 35% reduction in thickness occurs during the shell development in the glassblowing simulation. The thickness was evaluated at the highest point of the shell and normalized to the initial thickness. The shell radius was 4.5 mm, and the cavity volume was identical in all cases.

highest point in simulations for different initial thickness values. The normalized thickness demonstrated 25% to 35% reduction after glassblowing, Fig. 5. The thickness reduction was considered in the final design of the FQ die before glassblowing to achieve the designed operational frequency and frequency separation.

Although the shell thickness was assumed to be uniform in the parametric FE modal analysis, the thickness variation is inevitable in the glassblowing process since the deformation of the material is greater at the top of the shell than around the rim [8]. However, the design space provides an insight into the shell geometry design. For a more accurate estimation of the $n=2$ wineglass frequency and modal frequency separation, the glassblowing was simulated to predict the final geometry. Then, the final mesh was trimmed to remove the substrate region and transferred to the modal analysis to calculate the frequency of vibration modes of the shell. The comparison of the two methods revealed that the uniform thickness assumption resulted in lower $N=2$ and $N=3$ wineglass resonance frequencies.

V. EFFECT OF SHELL GEOMETRY ON THERMOELASTIC DAMPING (TED)

The geometry of shell impacts the Thermoelastic Damping (TED) of the resonator. Among the geometric parameters, thickness has the most significant effect on TED limit of the Q -factor in shell resonators [9]. The Q_{TED} of FQ shell resonators were derived from FE simulations for different thicknesses at three different diameters, Fig. 6. In all three cases, a minimum Q -factor occurred when the thickness was between $20\mu\text{m}$ and $30\mu\text{m}$, corresponding to the condition when the mechanical resonant frequency is close to the thermal eigenfrequency [10]. The quasi-isothermal condition in thinner shells and the quasi-adiabatic condition in thicker shells cause a weaker coupling between the strain field and the thermal field, reducing the energy dissipation through TED.

TABLE I

A SUBSET OF DESIGN COMBINATIONS FROM FIG. 4, CORRESPONDING TO $N=2$ WG FREQUENCY BETWEEN 4 TO 5 KHZ.

| Shell radius (mm) | Shell thickness (μm) | Anchor radius (mm) | $N=2$ WG Freq. (kHz) | Freq. separation (Hz) | Mode-ordering |
|-------------------|-----------------------------------|--------------------|----------------------|-----------------------|---------------|
| 5 | 60 | 0.3 | 4590 | 610 | Yes |
| 5 | 60 | 0.2 | 4511 | 756 | No |
| 5 | 60 | 0.4 | 4672 | 1338 | Yes |
| 4 | 40 | 0.3 | 4955 | 1996 | Yes |
| 4.5 | 40 | 0.4 | 4007 | 2244 | Yes |
| 4.5 | 40 | 0.6 | 4263 | 2869 | Yes |
| 4.5 | 40 | 1 | 4952 | 3800 | Yes |

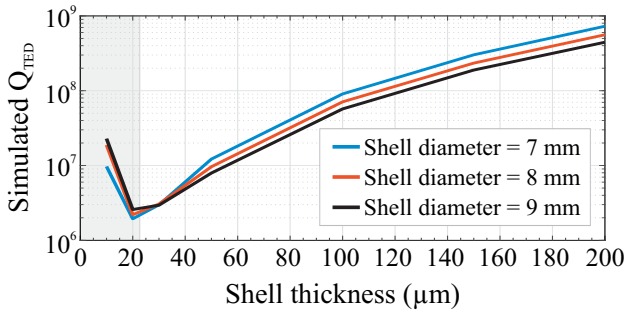


Fig. 6. Effect of shell thickness and diameter on the simulated Q_{TED} of hemi-toroidal shell resonators. The maximum TED was observed for the shell thickness in the range of $20\mu\text{m}$ to $30\mu\text{m}$.

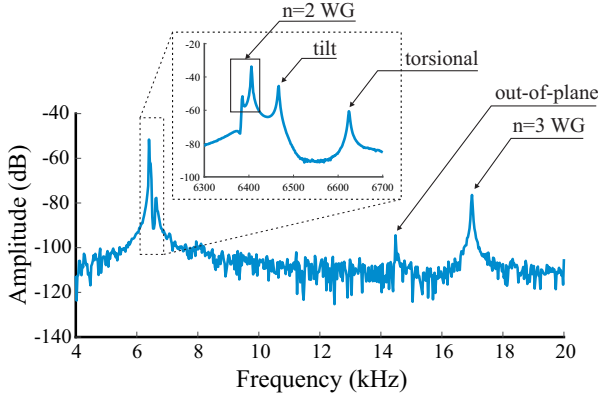


Fig. 7. An experimental frequency response of a shell resonator with $n=2$ WG resonance at 6.4 kHz, showing the proximity of spurious resonance mode to the operational mode in a non-optimized design (thickness = $80\mu\text{m}$, shell radius = 5 mm, and anchor radius = $400\mu\text{m}$).

VI. IDENTIFICATION OF RESONANCE MODES

The shell resonators were assembled on a piezo stack and mounted on a servo-motor controlled rotary stage. The amplitude of vibration was measured using a Laser Doppler Vibrometer (LDV) at incrementally spaced azimuth angles at every peak frequency, to identify the corresponding mode shapes [8]. Fig. 7 shows the experimental frequency sweep response of a shell resonator, demonstrating a proximity of the resonance modes, less than 200 Hz between $N=2$ WG and the tilt mode in a non-optimized design.

The frequency response of a shell with thickness = $45\mu\text{m}$, shell radius = 4.25 mm, and anchor radius = $500\mu\text{m}$ is shown in Fig. 8. The $N=2$ WG mode was identified at 5.7 kHz as the first vibration mode with a minimum frequency separation of 2 kHz to the nearest spurious mode (tilt). The experimental results demonstrated that frequency separation and mode-ordering could be achieved through the parameters of the shell geometry, at the operational frequency of interest.

VII. CONCLUSION

The design space exploration of hemi-toroidal shell resonators, considering the frequency scaling of the operational and spurious resonance modes, was performed. A parametric

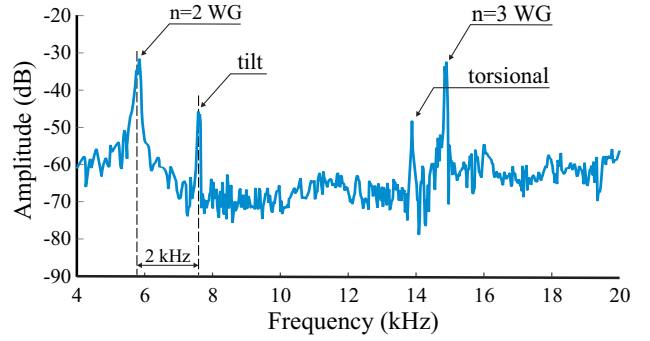


Fig. 8. A minimum frequency separation of 2 kHz was achieved between the $N=2$ WG and the closest resonance mode (tilt) in one of the design points, with thickness = $45\mu\text{m}$, shell radius = 4.25 mm, and anchor radius = $500\mu\text{m}$. The $N=2$ WG is the lowest resonance mode.

FE analysis of an approximated shell geometry provides the design space for a large number of data points. The data analysis demonstrated the feasibility of the design for a large frequency separation between the operational and spurious modes, allowing the ordering of resonance modes in low-frequency shell resonators. Two different geometries from the data points were fabricated and the separation of modal frequencies were demonstrated. The larger separation is anticipated to mitigate the energy dissipation through the mode coupling losses, and the mode-ordering would improve the environmental sensitivity characteristics of low-frequency shell resonator gyroscopes.

REFERENCES

- [1] D. M. Rozelle, "The hemispherical resonator gyro: From wineglass to the planets," in *Proc. 19th AAS/AIAA Space Flight Mechanics Meeting*, Savannah, Georgia, February, 2009.
- [2] D. Senkal, M. J. Ahamed, M. H. Asadian, S. Askari, and A. M. Shkel, "Demonstration of 1 million Q-factor on microglassblown wineglass resonators with out-of-plane electrostatic transduction," *IEEE Journal of Microelectromechanical Systems*, vol. 24, no. 1, pp. 29–37, 2015.
- [3] J. Y. Cho, J.-K. Woo, J. Yan, R. L. Peterson, and K. Najafi, "Fused-silica micro birdbath resonator gyroscope," *IEEE Journal of Microelectromechanical Systems*, vol. 23, no. 1, pp. 66–77, 2014.
- [4] M. H. Asadian, Y. Wang, and A. M. Shkel, "Design and fabrication of 3d fused quartz shell resonators for broad range of frequencies and increased decay time," in *IEEE Sensors Conference (SENSORS)*, New Delhi, India, October, 2018.
- [5] Y. Wang, M. H. Asadian, and A. M. Shkel, "Modeling the effect of imperfections in glassblown micro-wineglass fused quartz resonators," *Journal of Vibration and Acoustics*, vol. 139, no. 4, p. 040909, 2017.
- [6] D. Vatanparvar and A. M. Shkel, "Effect of fabrication imperfections on energy loss through mechanical mode coupling in mems," in *IEEE International Symposium on Inertial Sensors and Systems (INERTIAL)*, Lake Como, Italy, March, 2018.
- [7] M. H. Asadian, Y. Wang, S. Askari, and A. Shkel, "Controlled capacitive gaps for electrostatic actuation and tuning of 3d fused quartz micro wineglass resonator gyroscope," in *IEEE International Symposium on Inertial Sensors and Systems (INERTIAL)*, Kauai, HI, USA, March 2017.
- [8] Y. Wang, M. H. Asadian, and A. M. Shkel, "Compensation of frequency split by directional lapping in fused quartz micro wineglass resonators," *Journal of Micromechanics and Microengineering*, vol. 28, no. 9, p. 095001, 2018.
- [9] A. Darvishian, T. Nagourney, J. Y. Cho, B. Shiari, and K. Najafi, "Thermoelastic dissipation in micromachined birdbath shell resonators," *IEEE Journal of Microelectromechanical Systems*, vol. 26, no. 4, pp. 758–772, 2017.
- [10] C. Zener, "Internal friction in solids. i. theory of internal friction in reeds," *Physical review*, vol. 52, no. 3, p. 230, 1937.